This article has been accepted for publication in a future issue of this journal, but has not been fully edited. Content may change prior to final publication. Citation information: DOI 10.1109/TVT.2017.2661820, IEEE Transactions on Vehicular Technology

Power Quality Conditioning in Railway Electrification: A Comparative Study

Adel Tabakhpour, Andrea Mariscotti, *Senior Member, IEEE*, and Mohammad A. Abolhassani

***Abstract*—Electric transportation systems are a challenging load for three-phase transmission lines due to load variations, reactive power, imbalance and harmonic pollution. Many power quality conditioners and compensation technologies have been developed to ensure compatibility with power systems. The most important ones are investigated, identifying parameters and performances for comparison, including evaluation of cost and size. A reference case is used for simulation, focusing on three-phase current intensity, current rate of rise, DC link voltage, and dynamic response under various combinations of traction line load. The objective is to identify key characteristics supporting the selection of the appropriate compensation strategy for a new electrified railway system.**

***Index Terms*—Guideway transportation power systems, Power distribution, Power electronic converters, Power quality, Power system harmonics, Reactive power.**

I. Introduction

Railway electrification development has placed the rail transportation in a competitive position among transportation industries, due to its higher capacity, more reliable operation, less air pollution and less local CO_2 generation [1]. One of the key attributes of any new technology is the compatibility with the adjacent systems, for which requirements and constraints exist and the new technology shall comply with. Modern railways for medium and high speed use extensively the 25 kV 50/60 Hz supply scheme, tailored to considerable levels of traction power that may have significant impact on the utility; for this reason the Point of Common Coupling (PCC), where the three-phase utility is loaded, is normally located at a higher voltage level on the transmission system [2], rather than the distribution system. The traction system is single phase and the major impact on the utility is represented by uneven loading of phases, or, in other words, voltage imbalance and negative sequence components. Harmonic distortion is another relevant phenomenon, notwithstanding that modern rolling stock is equipped with front-end converters of the four-quadrant type with very efficient control of harmonics, waveshape and power factor [3]. Power quality in general represents a relevant set of requirements for modern electrical systems featuring larger nominal power levels and conversion frequencies [4].

Therefore, power quality must be considered in all aspects of the design for every system dealing with electric power systems. Many strategies have been proposed for power quality improvement in electric railways, investigated in [1] in a comprehensive historical perspective. Nowadays, power quality improvement strategies have developed to a mature degree for new electric railway systems, among which Railway static Power Conditioners (RPC) and its alternatives have the main place [5]. RPC consists of two single-phase back-to-back converters sharing a common DC-link capacitor, through which active and reactive power are applied (see Fig. 1(a)). The Active Power Quality Conditioner (APQC) was introduced [6, 7] as an alternative to RPC, with two less power-electronic switches, reducing the total cost of the compensator (see Fig. 1(b)); a Half-Bridge Railway Power quality Conditioner (HBRPC) was also proposed [8] saving two more power switches (see Fig. 1(c)).

These compensation schemes are based on the split of traction substation (TSS) secondary side into two sections, separated by section isolators implemented as catenary neutral sections. The pantograph crossing over the section isolator may produce arcs due to train current interruption; to avoid intense arcing, speed limitation is usually enforced at section isolators. Different schemes for co-phase supply systems were introduced [9-13], requiring no section isolators and removing speed limitation, thus suitable for high-speed lines.

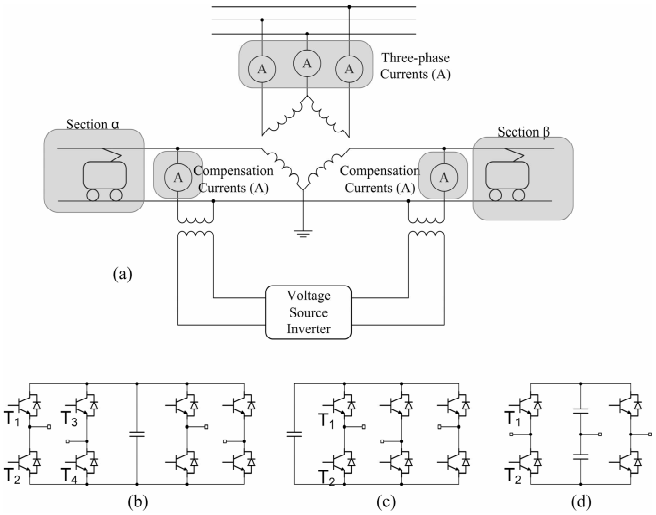

Fig. 1. Different compensation schemes, (a) general insertion scheme, (b) Railway Power Conditioner (RPC), (c) Active Power Quality Conditioner (APQC), (d) Half-Bridge Railway Power Conditioner (HBRPC)

In this paper these compensation schemes are compared for size and performance, starting from the common ground of same application and system parameters, and using always an optimized controller configuration for each compensator. A general loading scheme is used with either one or both left and right line sections loaded by an arbitrary nominal load, that is switched on and off at given time instants, in order to include the evaluation of the dynamic response of compensators and regulators. The objective is to identify advantages and disadvantages in terms of performance, number of active elements, sizing of elements and compensator.

This article has been accepted for publication in a future issue of this journal, but has not been fully edited. Content may change prior to final publication. Citation information: DOI 10.1109/TVT.2017.2661820, IEEE Transactions on Vehicular Technology

II. Railway Power Quality Conditioning

The most universal compensation schemes in electric railway are RPC and its alternatives (e.g. APQC, HBRPC, HPQC). These compensation schemes are connected to the TSS secondary, as shown in Fig. 1, and theoretically operate based on instantaneous active/reactive power theory, in which the three-phase currents at the TSS primary side are supposed to be: (i) three-phase symmetrical, (ii) fully sinusoidal with no relevant harmonic content, and (iii) aligned with the three-phase voltage featuring negligible reactive power. Thereafter, the difference between the load currents and the ideal currents must be generated by the compensator, called compensation currents. The compensator operates as an independent three-phase current source, generating the desired compensation currents.

Compensation currents can be calculated for a TSS with a V-V connection, based on the vector diagram shown in Fig. 2.

$$\begin{pmatrix} U_\alpha \\ U_\beta \end{pmatrix} = \begin{pmatrix} \bar{V} \angle -90 \\ \bar{V} \angle -30 \end{pmatrix} \tag{1}$$

As indicated in [7], sec. III.B, most of modern traction loads interface through 4-quadrant PWM-controlled converters, which generate negligible reactive power with a nearly unity power factor in each of the two single-phase sections. The load currents at the substation for the two sections decompose in three-phase current vectors that are not symmetrical and necessitate compensation of the respective lead and lag phase difference. So, moving from the secondary side to the primary side of the TSS transformer, reactive power changes and requires compensation despite the nearly unity power factor loads connected to the single-phase catenary system. In the following, to simplify calculations, one TSS section at a time is supposed to supply full load, whereas the other section is at no load; superposition of effects is then used to obtain a solution of general validity in all loading conditions.

The three-phase currents can be calculated from the load currents as in (2).

$$\begin{pmatrix} I_a \\ I_b \\ I_c \end{pmatrix} = \begin{pmatrix} aI_{Load} \\ 0 \\ -aI_{Load} \end{pmatrix} \tag{2}$$

$$I_{Load} = \bar{I} \angle -30 \tag{3}$$

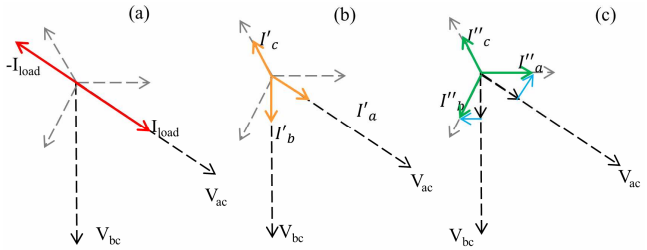

Fig. 2. Vector diagram of compensation currents based on instantaneous power theory, (a) before compensation, (b) after active power balancing, (c) after active and reactive power balancing

In (2), a is the transformation ratio of TSS, and $\bar{I}$ in (3) is the rms value of the train current. Assuming section β to be in no-load condition, the current of phase b is zero, and the currents of phases a and c are equal. To approach the symmetrical three-phase currents, one can draw half of the active current from the phase b. In this case, the amplitude of currents can be reduced to supply the same amount of load through two phases. Currents after active power balancing are shown in Fig. 2(b), corresponding to the terms in (4).

$$\begin{pmatrix} I_a' \\ I_b' \\ I_c \end{pmatrix} = \begin{pmatrix} \frac{a}{2}\bar{I} \angle -30 \\ \frac{a}{2}\bar{I} \angle -90 \\ \frac{\sqrt{3}}{2}a\bar{I} \angle 120 \end{pmatrix} \tag{4}$$

The active power between the two sections in (4) is balanced. With the amplitude of the two phase currents (in a and b) equal, for symmetrical three-phase currents, one must adjust the phase of these two currents to have 120° phase difference, as in Fig. 2(c). Having these two currents as $I_a'' = \frac{a}{\sqrt{3}}\bar{I}\angle 0$ and $I_b'' = \frac{a}{\sqrt{3}}\bar{I}\angle -120$, the current of the third phase can be obtained, as in (5).

$$\begin{pmatrix} I_a'' \\ I_b'' \\ I_c'' \end{pmatrix} = \begin{pmatrix} \frac{a}{\sqrt{3}}\bar{I}\angle 0 \\ \frac{a}{\sqrt{3}}\bar{I}\angle -120 \\ \frac{a}{\sqrt{3}}\bar{I}\angle 120 \end{pmatrix} \tag{5}$$

In (2)-(5), it was supposed that section β is at no load, and the current of section α is $\bar{I}$. To generalize the results, the currents of the two single-phase sections are considered $\bar{I}_\alpha$ and $\bar{I}_\beta$ (rms values), to obtain the full compensation currents for all loading conditions. By replacing $\bar{I}$ with $\bar{I}_\alpha + \bar{I}_\beta$ in (5), the total compensation currents can be obtained by superposition as in (6).

$$\begin{pmatrix} I_a'' \\ I_b'' \\ I_c'' \end{pmatrix} = \frac{a}{\sqrt{3}} \begin{pmatrix} (\bar{I}_\alpha + \bar{I}_\beta)\angle 0 \\ (\bar{I}_\alpha + \bar{I}_\beta)\angle 120 \\ (\bar{I}_\alpha + \bar{I}_\beta)\angle -120 \end{pmatrix} \tag{6}$$

Now, having the desired currents for each phase, one can obtain the switching pattern of the compensators (APQC, RPC, …) to get symmetrical three-phase currents.

Since the voltages of the two sections have 60° phase difference, one can define the active current, responsible for the active power, as in (7).

$$|I_{active}| = \frac{2}{\sqrt{3}}(\bar{I}_\alpha \times \sin(\omega t - 30) + \bar{I}_\beta \times \sin(\omega t - 90)) \tag{7}$$

This current represents the amplitude of fully compensated three-phase currents.

Therefore, the general control strategy is the same for all schemes, independent of the converter. The goal of the control unit is to achieve the exact amount of $|I_{active}|$, and then, to calculate the compensation currents as to have the same amplitudes as $|I_{active}|$. The details of obtaining the control unit is explained in [14], and the block diagram of the controller is shown in Fig. 3.

This article has been accepted for publication in a future issue of this journal, but has not been fully edited. Content may change prior to final publication. Citation information: DOI 10.1109/TVT.2017.2661820, IEEE Transactions on Vehicular Technology

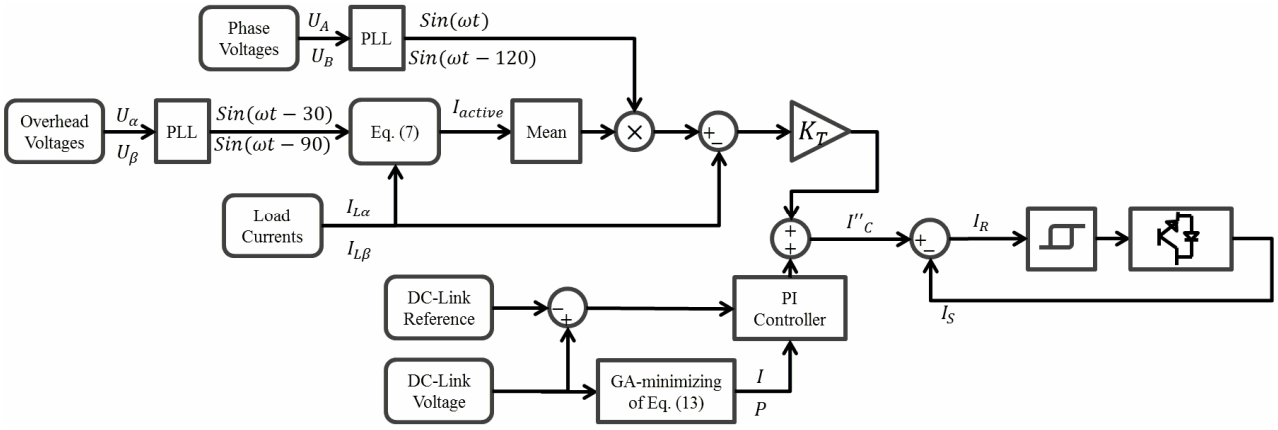

Fig. 3. Block diagram of the control unit for all compensation configurations with adaptive PI-controller parameters (PI-controllers are different for HBRPC)

III. Switch Control Signals

Compensation currents can be calculated by subtracting the load currents from the desired currents, with $I_c = -(I_a + I_b)$:

$$\begin{pmatrix} I_{Ca} \\ I_{Cb} \\ I_{Cc} \end{pmatrix} = \begin{pmatrix} I_a - I_a'' \\ I_b - I_b'' \\ I_c - I_c'' \end{pmatrix} \tag{8}$$

For all compensators with V-V connection at TSS, compensation currents are as in (8); however, switch control signals are different, depending on the inverter scheme.

$$\begin{pmatrix} I_{Ea} \\ I_{Eb} \\ I_{Ec} \end{pmatrix} = \begin{pmatrix} I_{Ca} - I_{Ca}^* \\ I_{Cb} - I_{Cb}^* \\ I_{Cc} - I_{Cc}^* \end{pmatrix} \tag{9}$$

The switch pulsating signals are derived from the *S* control quantity: error signals in (9) are compared using a hysteresis band *h*, generating switching pulses as controlled by *S*.

$$S = \begin{cases} T_1, T_4 & I_E < -h \\ T_2, T_3 & I_E > h \\ - & |I_E| \le h \end{cases} \tag{10}$$

When I_E is inside the hysteresis band, switches are kept in the previous state and this is indicated by the dash. The dc-link capacitor is charging when T_1 and T_4 are ON, discharging when T_2 and T_3 are ON. Switching pulses are generated as in (11), in which the said switches are ON (see Fig. 1(b)).

In APQC, there are three error signals and related control signals S_j (j=1,2,3) for brevity indicated as *S*, each of which controls two switches. When S=1, T_1 is ON and T_2 is OFF, and for S=0 *vice versa* (see Fig. 1(c)). Switching pulses for APQC are shown in (11).

$$S = \begin{cases} T_1 & I_E < -h \\ T_2 & I_E > h \\ - & |I_E| \le h \end{cases} \tag{11}$$

For the Half Bridge RPC (HBRPC), switching pulses are the same as for RPC (see Fig. 1(d)), but each control signal drives only two switches. Switching signals are generated as:

$$S = \begin{cases} T_1 & I_E < -h \\ T_2 & I_E > h \\ T_1 & |I_E| \le h \end{cases} \tag{12}$$

Switching pulses might be generated by other schemes, such as PWM; however, hysteresis band control as investigated in this work is usually preferred for its simplicity and quick response, besides keeping the average switching frequency to lower values, as well as switching power losses.

IV. Simulation and Analysis of Basic Compensators

A common system was chosen as case study, and then all three compensation schemes applied to implement the desired compensation. Results are reported for comparison and discussion of peculiar features of each scheme. The characteristics of the case study and of loading profiles of left and right sections are shown in Table I and Table II, respectively, which are kept the same for all simulations.

Compensators are compared using adaptive optimized PI regulators. The optimal values were identified using a genetic algorithm (GA) applied to the objective function of each problem defined below. Repeated optimizations and stability of the identified solution ensure that the identified regulator configuration is the optimal one (or very close to the optimum) for each configuration and that compensators are tested fairly at their best configuration and setting point.

TABLE I. Characteristics of the Railway System

Quantity	Value
Line Voltage	230 kV
Turns ratio of TSS transformer	230/27.5 kV
Supply Resistance	0.05 Ω
Supply Inductance	1 mH
Load Power (Trains' Total Power)	6 MW

TABLE II. Characteristics of the Railway Loads in Simulations

Time interval [s]	**0 – 0.1**	**0.1 – 0.2**	**0.2 – 0.4**	**0.4 – 0.6**
Left Section	Full Load		Full Load	No Load
Right Section	No Load		Full Load	Full Load
Compensator	Off	On		

This article has been accepted for publication in a future issue of this journal, but has not been fully edited. Content may change prior to final publication. Citation information: DOI 10.1109/TVT.2017.2661820, IEEE Transactions on Vehicular Technology

The adopted regulator controls the DC-link voltage (using the reference value shown in Table I) and positive and negative sequences (the reference for the positive sequence is given by the adopted load, while the negative is required to be zero). GA optimization was performed using the following objective function which takes into account all the mentioned quantities in (13) and is discussed in detail in [15].

$$J = w_1 \frac{J_1}{N_1} + w_2 \frac{J_2}{N_2} + w_3 \frac{J_3}{N_3} + w_4 \frac{J_4}{N_4} \tag{13}$$

with N_i normalizing scaling factors and w_i weights, for correct combination of sub-functions J_i.

$$J_1(V_{DC}) = \left(\frac{1}{T} \int_T (V_{DC} - V_{ref}) \right)^{1/2} \tag{14}$$

$$J_2(V_{DC}) = \max(V_{DC}) - \min(V_{DC}) \tag{15}$$

$$J_3(NSC) = \left(\frac{1}{T} \int_T (NSC)^2 \right)^{1/2} \tag{16}$$

$$J_4(PSC) = \left(\frac{1}{T} \int_T (PSC - PSC_{ref}) \right)^{1/2} \tag{17}$$

The operation of this optimum parameter adjustment can be understood from Fig. 3, where the GA optimization block receives the DC-link voltage, PSC (positive sequence component) and NSC (negative sequence component), and outputs the value of P and I parameters dynamically. This adaptive parameter adjustment of the PI-controller guarantees the efficient performance of the compensator, since these parameters depend on the loading conditions of the two sections, and in the long term they depend also on temperature, aging of components, etc. The optimized regulators minimize the rms error of the DC link voltage and of positive and negative sequence components, limiting also the maximum excursion of DC link voltage during transients.

A. Compensation of System with RPC

The RPC in Fig. 1(a) has 8 power switches arranged in 2 back-to-back converters, by which compensation currents are separately generated. The compensated primary three-phase currents, and NSC and PSC are shown in Fig. 4(a) and (b), respectively. The dynamic performance of the system is slow, compared to other compensators; in general, however, a time response shorter than 1 s may be considered a good dynamic behavior for a railway system compensator. The DC-link voltage in Fig. 4(c) reveals the dynamic response at each transition between states at t=0.1, 0.2 and 0.4 s. RPC performance is highly influenced by DC-link voltage [16], that shall be controlled and kept as constant as possible.

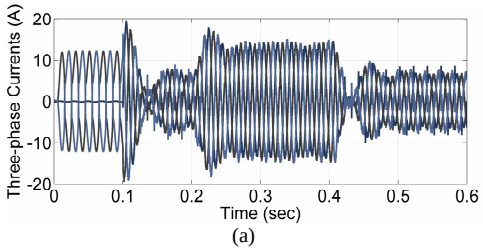

(a)

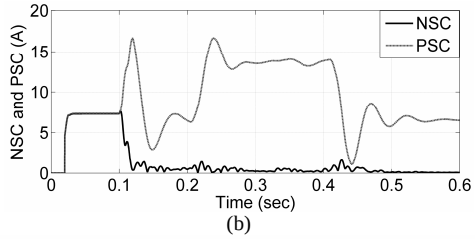

(b)

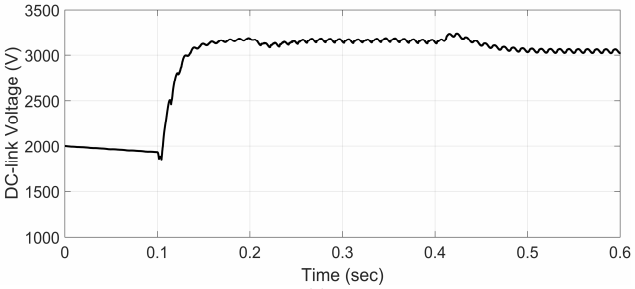

(c)

Fig. 4. With the Compensation of RPC (a) Three-phase currents of TSS primary side (b) PSC and NSC of currents (c) DC-link voltage waveform

Compensation currents shown in Fig. 5(a) are important for design and to size power switches. In RPC, the outer legs generate the compensation currents for phase A and B, respectively; the two inner legs together generate that of phase C. Therefore, the switches for phase A and B are the most stressed and those currents determine the switch rating. In the case study appearing in this paper power switches must be sized for a rated current of 4100 A, as from Fig. 5(a).

Another determining design parameter for switches is the voltage stress, to be compared to the switch nominal voltage with adequate margin and related to the current derivative through an estimate of the total stray inductance (also when using snubbers). Stray inductance L is of course approximate and its value is left undetermined: the comparison between solutions is based solely on current derivative, provided that stray inductance is approximately the same for all architectures, since it is influenced by the geometry of the single power switch and its auxiliary circuits.

$$V_{stress} = L \frac{di_L}{dt} \tag{14}$$

In Fig. 5(b) the derivative is as large as 3800 kA/s for RPC.

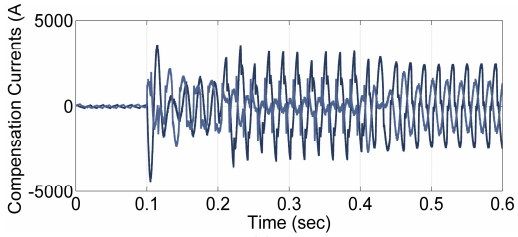

(a)

This article has been accepted for publication in a future issue of this journal, but has not been fully edited. Content may change prior to final publication. Citation information: DOI 10.1109/TVT.2017.2661820, IEEE Transactions on Vehicular Technology

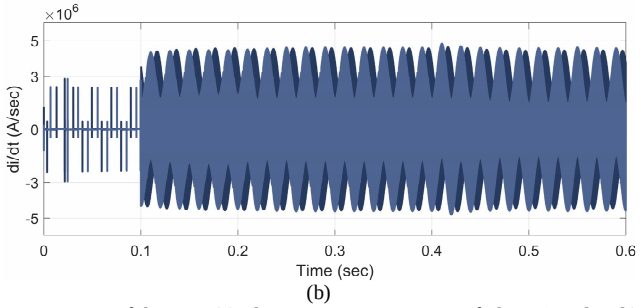

(b)

Fig. 5. Sizing of the RPC (a) The compensation current of Phase A and B (b) Compensation current derivatives with respect to time

B. *Compensation of System with APQC*

The Active PQC (APQC) has 6 power switches arranged as an independent three-phase current source. It considers the two single-phase sections as a series unbalanced three-phase load and generates compensation currents to have symmetrical currents, including harmonics and reactive power compensation. The APQC compensated primary three-phase currents, NSC and PSC are shown in Fig. 6(a) and (b). Dynamic performance in Fig. 6(c) is far better than for RPC.

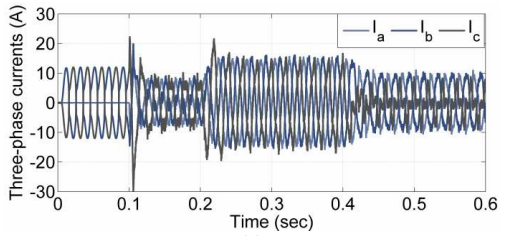

(a)

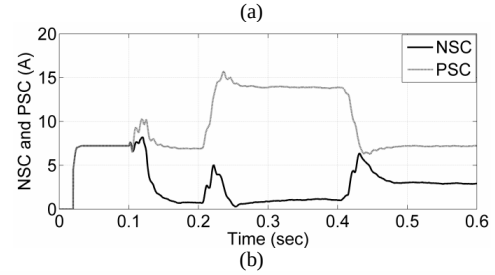

(b)

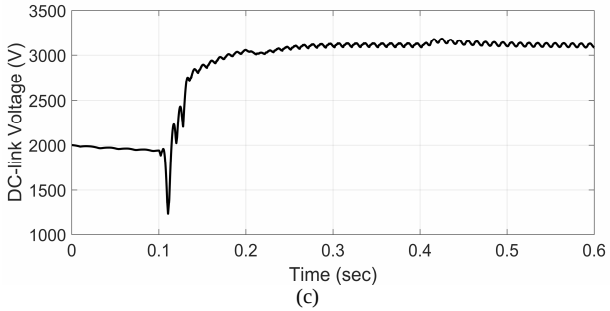

(c)

Fig. 6. With the Compensation of APQC (a) Three-phase currents of TSS primary side (b) PSC and NSC of currents (c) DC-link voltage waveform

Compensation currents and current derivative for power switch voltage stress are shown in Fig. 7: current rating is the same as for RPC.

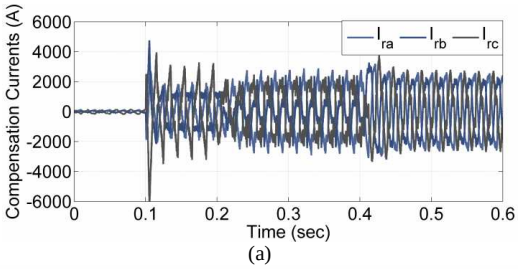

(a)

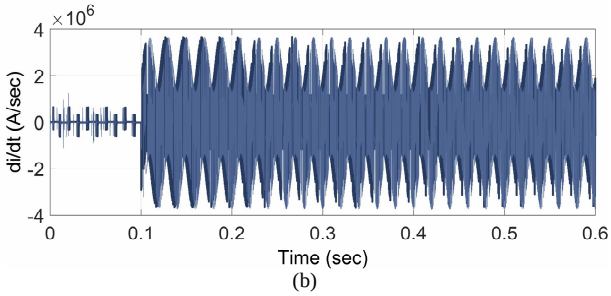

(b)

Fig. 7. Sizing of the APQC (a) The three-phase compensation current (b) Compensation current derivatives with respect to time

C. *Compensation of System with HBRPC*

The HBRPC generates compensation currents by controlling 4 power switches. One feedback loop has to be added to the control system to keep constant the voltage of the neutral point between the two capacitors: the DC-link voltage controller in HBRPC has thus two feedback loops with two PI-controllers, as shown in Fig. 8. The inner loop controls DC-link capacitor voltages by summing and comparing to reference voltage; the outer loop keeps the DC-link neutral point at zero by comparing the two capacitor voltages (subtraction).

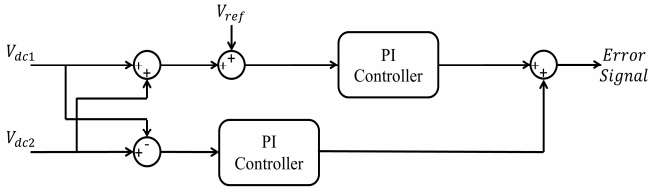

Fig. 8. Double-loop control of the DC-link capacitors in HBRPC

As it will be shown below, the voltage stress on HBRPC power switches is 5 times that of APQC or RPC; therefore, the DC-link capacitor value in this scheme is usually selected at least 50% larger than for APQC. However, in this study the DC-link capacitor has been selected exactly the same as the other compensators in order to compare them in the same conditions.

The primary side three-phase currents and the NSC and PSC of current are shown in Fig. 9(a) and (b). HBRPC dynamics are fast, as shown by the DC-link voltage profile in Fig. 9(c): the steady state is reached in less than 2 cycles.

This article has been accepted for publication in a future issue of this journal, but has not been fully edited. Content may change prior to final publication. Citation information: DOI 10.1109/TVT.2017.2661820, IEEE Transactions on Vehicular Technology

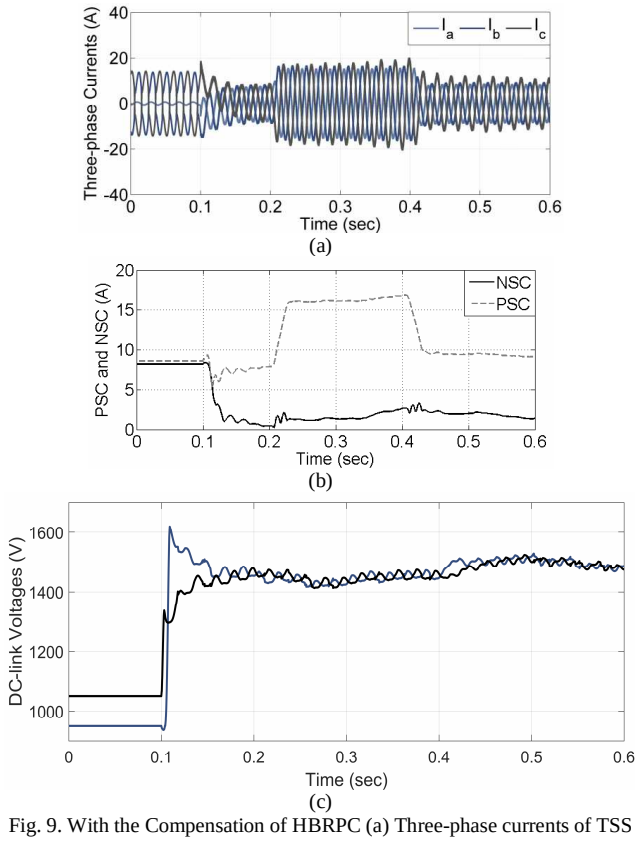

Fig. 9. With the Compensation of HBRPC (a) Three-phase currents of TSS primary side (b) PSC and NSC of currents (c) DC-link voltage waveform

Compensation currents are the same of APQC and RPC, as shown in Fig. 10(a); however, the voltage stress on switches is about five times that of RPC and APQC (Fig. 10(b)).

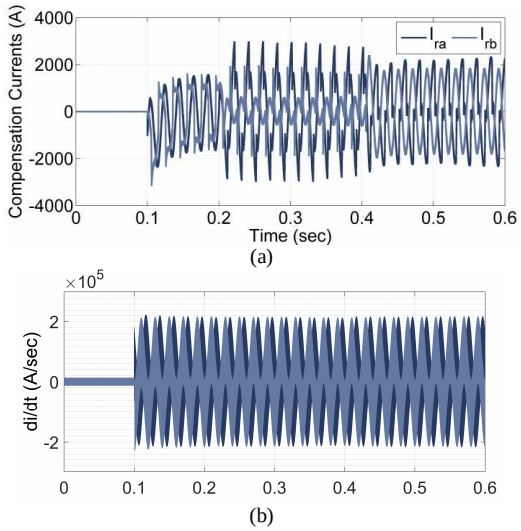

Fig. 10. Sizing of the HBRPC (a) The three-phase compensation current (b) Compensation current derivatives with respect to time

Selecting a larger DC link capacitor or setting a larger nominal DC link voltage increases the available power, injecting more power at each switching event and thus requiring a lower switching frequency, reducing in turn the current derivative and voltage stress on power switches. A tradeoff is therefore necessary between switch stress, size of capacitor bank and HBRPC compensator, and cost.

V. Hybrid Power Quality Conditioner

The compensation schemes reviewed in the previous section are conventional ones for power quality conditioners. Heuristic methods and various combinations have been proposed keeping the compensation methods conventional [14, 17-21]. The hybrid power quality conditioner (HPQC) [14, 22] is a combination of an APQC with a static VAr compensator (SVC), as shown in Fig. 11, to improve system performance and reduce power switch rating. The performance improvement for SVC was investigated in [23].

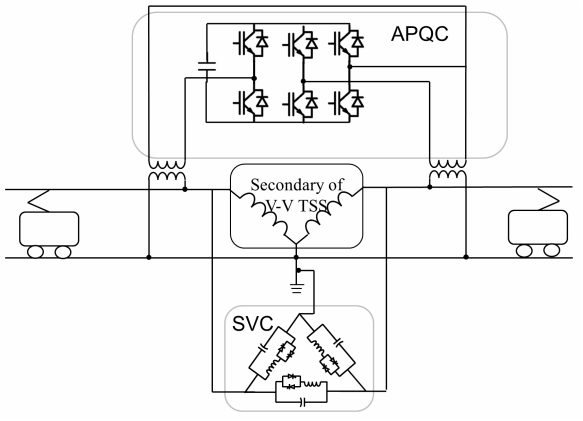

Fig. 11. Hybrid power quality conditioner [14]

HPQC performance is far better than the other schemes (see Fig. 12(c)), and the total cost of the system would be lower for high-power TSSs. However, the HPQC has an extra unit, the SVC, which may occupy additional space and might not be appropriate for subway TSSs, where space is at premium.

HPQC control unit is similar to the conventional APQC, with the NSC compensated by the SVC (see Fig. 12).

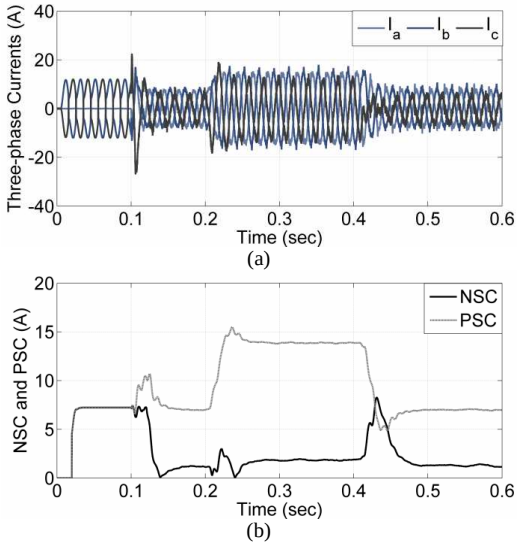

This article has been accepted for publication in a future issue of this journal, but has not been fully edited. Content may change prior to final publication. Citation information: DOI 10.1109/TVT.2017.2661820, IEEE Transactions on Vehicular Technology

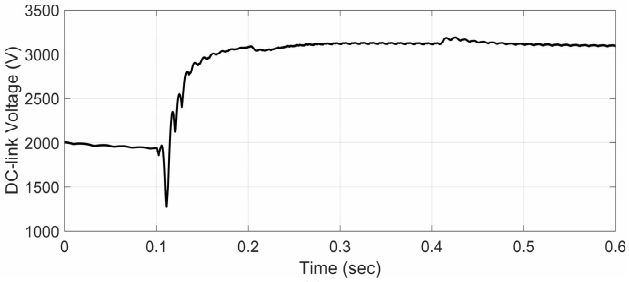

(c)

Fig. 12. With the Compensation of HPQC (a) Three-phase currents of TSS primary side (b) PSC and NSC of currents (c) DC-link voltage waveform

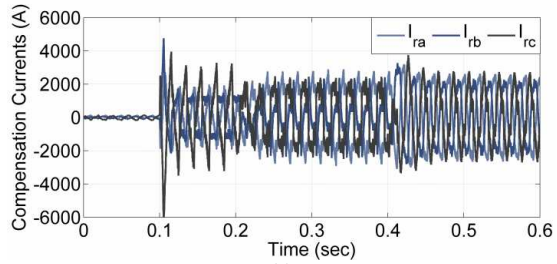

(a)

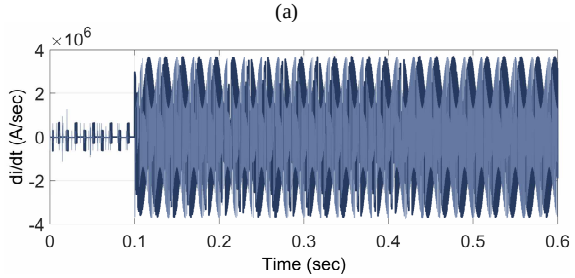

(b)

Fig. 13. Sizing of the HPQC (a) The three-phase compensation current (b) Compensation current derivatives with respect to time

The DC-link capacitor in this scheme is selected to be 15 mF, which is less than half that of APQC and RPC, simply because most of the current compensation is done by the SVC. In this case, the APQC acts as an active filter, mostly taking care of harmonics, therefore, the capacitor voltage level or capacitance, can be reduced in order to decrease the total costs. In this paper, the voltage level of the DC-link is selected the same other schemes, and the DC-link capacitance is reduced to show the efficiency of this combination.

The compensation methods investigated so far are compared in terms of key characteristics in Table III. However, an additional scheme is considered that distinguishes for the adopted insertion scheme.

VI. CO-PHASE COMPENSATOR

Section isolators force a speed limitation on the speed profile of railway lines. The co-phase TSS does not need section isolators at the TSS as shown in Fig. 14, halving their number. This feature has made the co-phase supply system an appropriate choice for high-speed railway lines; however, the power switches are working at the maximum currents in all load conditions. The co-phase supply system operates as a traditional compensation system, in which the total load is supplied through one phase and the other phase has no load. The inverter draws half of the total current from the unloaded phase to balance the load between the other two phases. An APQC was selected in this work as active power conditioner (APC) in the co-phase scheme (see Fig. 14).

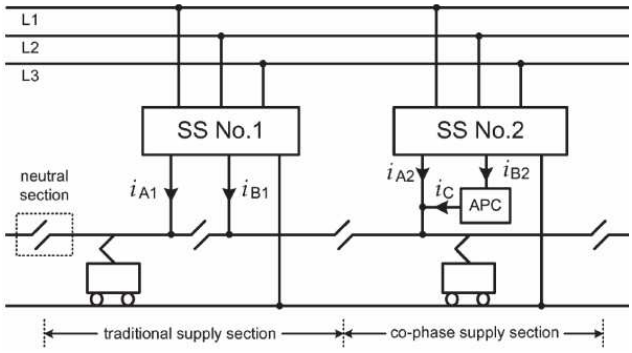

Fig. 14. Co-phase supply system at SS no. 2 compared with the traditional supply system at SS no. 1 [12]

In the co-phase supply system the overhead contact wire is supplied by just one single-phase of TSS secondary ; therefore, when the train crosses and passes the TSS, it has no influence on the three-phase currents at the primary side, as shown in Fig. 15(a). The NSC and PSC of current can be seen in Fig. 15(b), where the two peaks of NSC at the beginning of the each sub-interval are similar to the APQC ones and may be justified observing that the whole power is supplied through a single phase of the three-phase system. The DC-link voltage shown in Fig. 15(c) is quite stable even if with a significant ripple at 100 Hz.

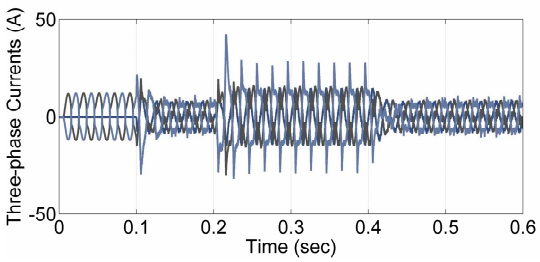

(a)

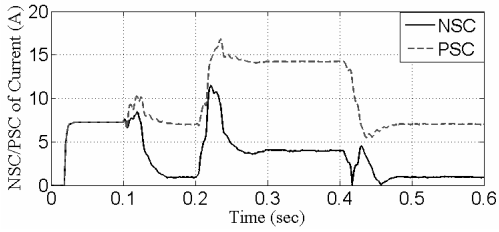

(b)

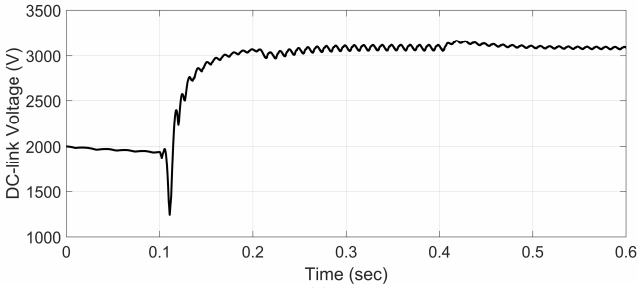

(c)

Fig. 15. With the Compensation of co-phase system (a) three-phase currents of TSS primary side (b) PSC and NSC of currents (c) DC-link voltage

This article has been accepted for publication in a future issue of this journal, but has not been fully edited. Content may change prior to final publication. Citation information: DOI 10.1109/TVT.2017.2661820, IEEE Transactions on Vehicular Technology

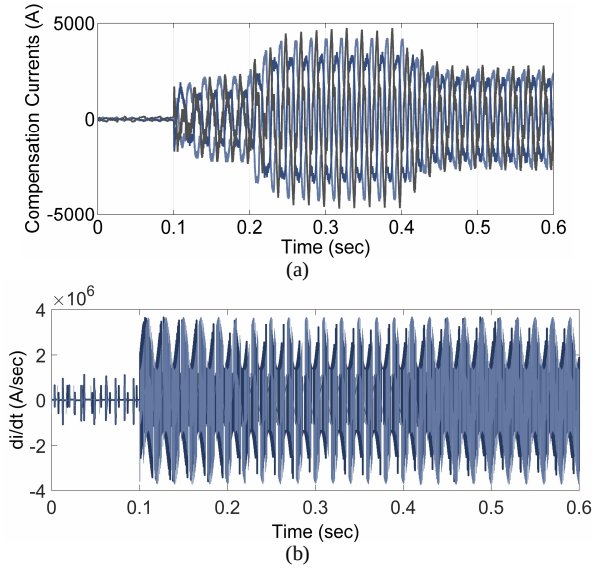

Fig. 16. Sizing of the co-phase system (a) The three-phase compensation current (b) Compensation current derivative with respect to time

There are also theoretically proven schemes in co-phase systems [13], in which the section isolators are eliminated throughout the railway line, however, this scheme faces a serious problem: the whole power is supplied through the power electronic converters; for a real-scale railway system, it would require power electronic switches that are presently not feasible, asking a long way to become practical in railway industry. Other co-phase systems follow the scheme in Fig. 17, combining active and passive component. The most important advantage of the co-phase system is that this scheme eliminates the section isolators in the co-phase connected TSS, which could prevent the practical and operational problems associated with the section isolators [1]. A general evaluation of the co-phase systems are presented in [1], where the most important co-phase systems [9-13, 24] are discussed.

TABLE III. CHARACTERISTICS OF THE ANALYZED COMPENSATORS

Compens. scheme	**Num. of switches**	**DC-link capacitor**	$\frac{NSC}{PSC}$%	**Compens. current [A]**	$\frac{di}{dt}$[kA/s]	**Resp. time [cycles]**	**Max DC-link voltage [V]**	**Notes**
RPC	8	40 mF	1 - 6	4100	3800	1	3200	
APQC	6	40 mF	5.5 – 11	3900	3800	1	3080	
HBRPC	4	2 × 60 mF	6.7 – 10.5	4000	20000	2.5	3110	Two-loop DC-link voltage controller.
HPQC	6	15 mF	6.5 - 10	1900	3800	1	3080	HPQC has 6 extra thyristors, 3 capacitors and 3 inductors.
Co-phase with APQC	6	40 mF	5 - 26	3900	3800	1	3080	Co-phase system can also adopt the other compensators.

VII. COMPENSATORS COMPARISON

Among the railway power quality conditioners the APQC is preferred to RPC, ensuring the same performance with two less switches, and a simpler control unit. HBRPC has nearly the same performance with only 4 switching devices. However, it needs a bilateral DC-link voltage with a double-loop feedback control unit to control the two DC-link voltages. Moreover, HBRPC switching devices shall be sized to tolerate a higher current derivative, definitely requiring more expensive devices (at such high rated voltage values, increasing it further is extremely expensive). Two less switches are not the only factor determining the overall cost of the bridge, if it is observed that the APQC has the structure of the three-phase inverter, which is quite commonplace and is being manufactured in large numbers, favorably impacting on the final price.

For DC link sizing, in the considered examples most of compensators use a 40 mF capacitor bank; the HPQC has a smaller bank because part of the energy is related to the added filters of the Static VAr Compensator, while for the HBRPC a slightly oversized double bank is compulsory. HBRPC is probably also seen as less reliable for concerns related to the stability of the two DC links.

Peak and average compensation current intensity and current derivative influence the sizing of the coupling single-phase transformers as for magnetization, copper cross section and losses. The HBRPC has the smallest compensation current peak value and in general average intensity, requiring the smallest coupling transformer.

The co-phase system is usually preferred in high-speed lines because it does not need section isolators at TSSs. The compensator is fully loaded in the co-phase system, because its structure is like a traditional scheme supplied through only one single-phase section (that embraces left and right line portions), leaving the other section at no load (see Fig. 17 where the co-phase system is redrawn). This increases of course the utilization percentage of switching devices. However, the control unit is simpler in this scheme.

This article has been accepted for publication in a future issue of this journal, but has not been fully edited. Content may change prior to final publication. Citation information: DOI 10.1109/TVT.2017.2661820, IEEE Transactions on Vehicular Technology

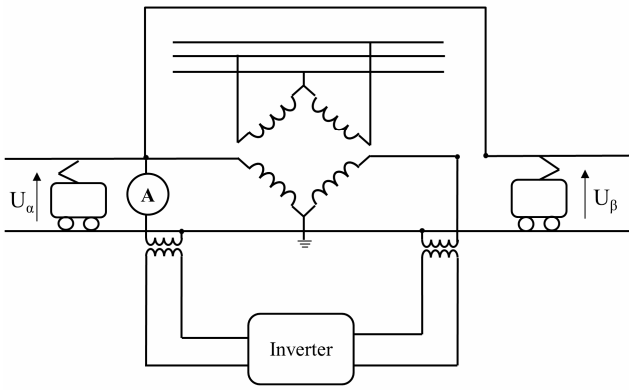

Fig. 17. Co-phase system inserted in a traditional compensation scheme

The HPQC can also be a good choice for example in two cases: in high-capacity TSSs, when traditional conditioners may be infeasible due to the high rating required for power switches; for critical TSSs, such as TSSs far from the point of common coupling with a low short-circuit power level and/or near susceptible loads, because it was shown that HPQC has the best performance among the studied compensation methods. However, it must be considered that the introduced HPQC embeds an additional complete SVC, which includes three capacitors, three inductors, and six thyristors, and a simple dedicated controller. Although its performance is the best among other schemes, it is more expensive and requires more space, especially for the additional SVC.

The advantages and disadvantages of all these schemes are summarized in Table IV, where the most important features of each strategy are summarized.

TABLE IV. ADVANTAGES/DISADVANTAGES OF COMPENSATORS

Compens. scheme	Advantages			Disadvantages			Additional Features
	Performance	Reliability	Maintainability	Total Cost	Control Complexity	Space Utilization	
RPC	**	**	**	***	***	***	
APQC	**	***	***	**	**	**	
HBRPC	*	****	****	*	****	*	Least total cost
HPQC	***	*	*	****	***	*****	Best performance
Co-phase with APQC	**	***	***	**	**	**	Less section isolators

Note. More asterisks demonstrate more relative advantages in the first three columns and more relative disadvantages in second three columns.

VIII. CONCLUSION

The problem of the impact of 25 kV electric railways on the utility grid and its compensation was considered focusing on static compensator architectures and insertion schemes. Compensator characteristics have been synthesized in terms of effectiveness of compensation on the utility three-phase current, transient response and stability of internal quantities, size and complexity in terms of number of active devices, capacitive storage requirements and additional external devices. The following railway power quality conditioners have been considered: RPC, APQC, HBRPC, HPQC, and co-phase; besides the mentioned compensation of current (and voltage) imbalance, these compensators can address Power Quality issues in general, including harmonic distortion mitigation and compensation.

For comparison all compensators are controlled by a Proportional-Integral PI regulator, whose parameters have been case by case optimized using a genetic algorithm applied to an all-comprehensive objective function, ensuring that each compensator is simulated at its best in terms of compensation performance. The results consist in the positive and negative sequence components of the three-phase current, the DC-link voltage, the intensity of required compensation currents and their derivative, the latter put in relationship to the voltage stress onto semiconductor power switches, and as a consequence possibly increased voltage rating. The number of necessary active power, storage and external devices gives an immediate estimate of size and cost.

The APQC has proven to be a comprehensive compensator with many advantages; however, for high-speed railway systems Co-Phase systems may be preferred due to the lack of section isolators at TSSs. Moreover, in some special cases, such as very high capacity TSSs, hybrid compensators have been proved to be appropriate.

ACKNOWLEDGMENT

The authors gratefully appreciate the valuable help and support of Dr. Alfred Baghramian and Dr. Siamak Farshad.

REFERENCES

[1] S.M.M. Gazafrudi, A. Tabakhpour Langerudy, E.F. Fuchs, and K. Al-Haddad, “Power Quality Issues in Railway Electrification: A Comprehensive Perspective,” IEEE Trans. Ind. Electron., vol. 62, pp. 3081-3090, 2015.

[2] C. Shi-Lin, R.J. Li, and H. Pao-Hsiang, “Traction system unbalance problem-analysis methodologies,” IEEE Trans. Power Del., vol. 19, pp. 1877-1883, 2004.

[3] R. Barnes and K.T. Wong, “Unbalance and harmonic studies for the Channel Tunnel railway system,” IEE Proc. B Electric Power Appl., vol. 138, pp. 41-50, 1991.

[4] A. Mariscotti, “Measuring and Analyzing Power Quality in Electric Traction Systems,” Int. J. Measur. Tech. Instrum.. Eng., vol. 2, pp. 21-42, 2012.

[5] H. Morimoto, M. Ando, Y. Mochinaga, T. Kato, J. Yoshizawa, T. Gomi, et al., “Development of railway static power conditioner used at substation for Shinkansen,” Proc. Power Conv. Conf., 2002, vol. 3, pp. 1108-1111.

[6] S. Zhuo, J. Xinjian, Z. Dongqi, and Z. Guixin, "A novel active power quality compensator topology for electrified railway," IEEE Trans. Power Electron., vol. 19, pp. 1036-1042, 2004.
[7] W. Chuanping, L. An, J. Shen, M. Fu Jun, and P. Shuangjian, "A Negative Sequence Compensation Method Based on a Two-Phase Three-Wire Converter for a High-Speed Railway Traction Power Supply System," IEEE Trans. Power Electron., vol. 27, pp. 706-717, 2012.
[8] M. Fujun, L. An, X. Xianyong, X. Huagen, W. Chuanping, and W. Wen, "A Simplified Power Conditioner Based on Half-Bridge Converter for High-Speed Railway System," IEEE Trans. Ind Electron., vol. 60, pp. 728-738, 2013.
[9] S. Zeliang, X. Shaofeng, and L. Qunzhan, "Single-Phase Back-To-Back Converter for Active Power Balancing, Reactive Power Compensation, and Harmonic Filtering in Traction Power System," IEEE Trans. Power Electron., vol. 26, pp. 334-343, 2011.
[10] N.Y. Dai, K.W. Lao, M.C. Wong, and C.K. Wong, "Hybrid power quality conditioner for co-phase power supply system in electrified railway," IET Power Electron., vol. 5, pp. 1084-1094, 2012.
[11] K.W. Lao, N. Dai, W.G. Liu, and M.C. Wong, "Hybrid Power Quality Compensator With Minimum DC Operation Voltage Design for High-Speed Traction Power Systems," IEEE Trans. Power Electron., vol. 28, pp. 2024-2036, 2013.
[12] S. Zeliang, X. Shaofeng, L. Ke, Z. Yuanzhe, N. Xiaoqiang, Q. Daqiang, et al., "Digital Detection, Control, and Distribution System for Co-Phase Traction Power Supply Application," IEEE Trans. Ind Electron., vol. 60, pp. 1831-1839, 2013.
[13] H. Xiaoqiong, S. Zeliang, P. Xu, Z. Qi, Z. Yingying, Z. Qijun, et al., "Advanced Cophase Traction Power Supply System Based on Three-Phase to Single-Phase Converter," IEEE Trans. Power Electron., vol. 29, pp. 5323-5333, 2014.
[14] A. Tabakhpour and S. Mousavi, "Hybrid railway power quality conditioner for high-capacity traction substation with auto-tuned DC-link controller," IET Elec. Syst. Transport. Available, vol. 6, n. 3, Sept. 2016, p. 207-214.
[15] A. Tabakhpour and A. Mariscotti, "Tuning of a railway power quality conditioner," 18th Mediterranean Electrotechnical Conference (MELECON), 2016, pp. 1-7.
[16] A. Mariscotti, "Analysis of the DC-link current spectrum in voltage source inverters," IEEE Trans. Circuit. Syst. I: Fundamental Theory Appl., vol. 49, pp. 484-491, 2002.
[17] L. An, P. Shuangjian, W. Chuanping, W. Jingbing, and S. Zhikang, "Power Electronic Hybrid System for Load Balancing Compensation and Frequency-Selective Harmonic Suppression," IEEE Trans. Ind Electron., vol. 59, pp. 723-732, 2012.
[18] B. Biswal, M. Biswal, S. Mishra, and R. Jalaja, "Automatic Classification of Power Quality Events Using Balanced Neural Tree," IEEE Trans. Ind Electron., vol. 61, pp. 521-530, 2014.
[19] V.F. Corasaniti, M.B. Barbieri, P.L. Arnera, and M.I. Valla, "Hybrid Active Filter for Reactive and Harmonics Compensation in a Distribution Network," IEEE Trans. Ind Electron., vol. 56, pp. 670-677, 2009.
[20] K.W. Lao, M.C. Wong, N. Dai, C.K. Wong and C.S. Lam, "A Systematic Approach to Hybrid Railway Power Conditioner Design with Harmonic Compensation for High-Speed Railway," IEEE Trans. Ind Electron., vol. 62, n. 2, pp. 930-942, Feb. 2015.
[21] S. Rahmani, A. Hamadi, K. Al-Haddad, and L.A. Dessaint, "A Combination of Shunt Hybrid Power Filter and Thyristor-Controlled Reactor for Power Quality," IEEE Trans. Ind Electron., vol. 61, pp. 2152-2164, 2014.
[22] S.M.M. Gazafrudi and A. Tabakhpour Langerudy, "Hybrid Power Quality Conditioner Installed in a Traction Substation With Optimized DC-Link Voltage," Int. Conf. Advanced Railway Engineering, Istanbul, Turkey, 2015.
[23] S.V. Raygani, A. Tahavorgar, S.S. Fazel, and B. Moaveni, "Load flow analysis and future development study for an AC electric railway," IET Elec. Syst. Transport., vol. 2, pp. 139-147, 2012.
[24] K.W. Lao, M.C. Wong, N. Dai, C.K. Wong, and C.S. Lam, "A Systematic Approach to Hybrid Railway Power Conditioner Design With Harmonic Compensation for High-Speed Railway," IEEE Trans. Ind. Electron., vol. 62, pp. 930-942, 2015.